OPERATIONAL REVIEW AND ANALYSIS OF THE S3T SURVEILLANCE RADAR

Cristina Pérez Hernández[1], Maria Antonia Ramos Prada[1] Marco Alessandrini[2], David Cano Mañanes[3], Jan Siminski[2], Fabio Pelorossi[2], Piermario Besso[2], Gian Maria Pinna[3], Rafael Casado Gómez[4], Jacobo Martínez-Villa Salmerón[4], Carlos Javier Lluch Jouy[4], Guillermo Ojeda Rodriguez[4], Pablo Íñiguez Cano[4], Esperanza Maria Lao Amores[4]

[1] CDTI, C/ Cid 4, 28001 Madrid, Spain
Email: {cristina.perez, mariaantonia.ramos} @cdti.es

[2] ESA/ESOC, Robert-Bosch-Str. 5, 64293 Darmstadt, Germany
Email: {Marco.Alessandrini, Jan.Siminski, Fabio.Pelorossi, Pier.Mario.Besso}@esa.int

[3] ESA/ESAC, Camino bajo del Castillo, 28692 Villanueva de la Cañada, Madrid, Spain
Email: {David.Cano.Mananes, GianMaria.Pinna}@esa.int

[4] Indra Sistemas, Crta Loeches 9, 28850 Torrejón de Ardoz, Madrid, Spain
Email: {rcasado, jmartinezv, clluch, gojeda, piniguez, emlao}@indra.es

ABSTRACT

The Spanish Space Surveillance and Tracking Surveillance Radar (S3TSR) is a radar system developed by Indra within a project technically followed by ESA and funded by the Spanish Administration through CDTI management. It is a ground-based radar in close monostatic configuration, operating at L-band and capable of providing positional information of orbital objects. The radar provides automatic surveillance and tracking of space objects in Low Earth Orbit (LEO), from 200 km to 2000 km of orbit height above Earth. This is performed by continuously scanning the instrumented Field of Regard (FoR), generating track reports for all detected objects. Surveillance and tracking of LEO objects are activities with increasing strategic value, essential to perform conjunction analysis and to provide services such as collision avoidance and fragmentation and prevent further debris generation.

The S3TSR is operated 24x7 since early 2019 and is providing high accuracy tracks to the Spanish Space Surveillance and Tracking Operation Centre (S3TOC), where they are used to maintain a catalogue of currently more than 2400 LEO objects and to generate autonomous conjunction analysis products.

This paper will highlight the measured performance of the S3TSR, comparing them versus the expected performance according to the design of the radar, and provide some of the results from the analysis of the operational data.

The paper will present the analysis of the range and angular position of the objects detected, as well as the objects' Radar Cross Section (RCS) derived from the Signal To Noise Ratio (SNR) measured by the radar.

After more than two years in operation, an overview of the performances and the S3TSR contribution to safeguard the space environment will be presented assessing the powerful potential the S3TSR has with its scalability design.

1 INTRODUCTION

CDTI is coordinating the development and operations of the Spanish Space Surveillance and Tracking (S3T) system in collaboration with the Spanish Ministry of Defence, among others. In addition, the European Space Agency (ESA) is supporting CDTI in the development and procurement of the S3T System, via industrial contracts awarded to the Spanish Industry.

The S3T Surveillance Radar (S3TSR) has been developed by Indra under the frame of the S3T project. The S3TSR is specifically designed for the detection of space debris in the LEO orbital regime (200-2000 km). It is an advanced scalable radar developed in Europe, by European industry, with full European know-how and key European technologies.

It has been designed and developed with scalability as main concept, allowing an easy, steady and cost-effective growth in size, power and performances.

The S3TSR entered operations in February 2019 using its first version configuration of one transmitter (Tx) and one receiver (Rx)

Since then, it's providing measurements of very high

Proc. 8th European Conference on Space Debris (virtual), Darmstadt, Germany, 20–23 April 2021, published by the ESA Space Debris Office
Ed. T. Flohrer, S. Lemmens & F. Schmitz, (http://conference.sdo.esoc.esa.int, May 2021)

quality to the S3TOC (Spanish SST Operations Center) and supporting the generation and maintenance of the S3T catalogue of space debris.

Figure 1: S3TSR transmitter antenna.

2 S3TSR DESCRIPTION

The S3TSR is a close-monostatic ground-based pulse radar system consisting in a transmitting antenna and a receiving antenna operating at L band and capable of providing positional information of orbital objects by means of space surveillance

The transmitting subsystem is based on a distributed transmitter architecture, composed of a number of identical solid-state modules. This approach enhances the maintainability of the system and allows soft degradation of the system performance in presence of any transmitter faults. The amplifiers are based on the latest technology GaN transistors, which offer much higher reliability and efficiency figures (lower power consumption) than conventional LDMOS transistors.

The receiving subsystem is based on a single replicated active module that performs reception and beamforming.

Rx and Tx Antennas are composed of identical building blocks (sub-arrays) attached to a supporting structure. The interconnection is based on a small number of cables.

The architecture design provides soft-fail feature in most antenna components (the failure of units does not produce system off state but only minor degradation in performances). For critical components with high replacement time, complete redundancy is provided.

Recording and analysis tools, which are included in the Monitoring Console Workstation (MCS), present and facilitate the validation and periodic maintenance of the radar system.

Figure 2. S3TSR Radar at Morón de la Frontera A.B (Seville, Spain)

3 ACCURACY PERFORMANCE

The validation of the accuracy of the radar measurements is based on having precise orbits of objects that can be detected by the S3TSR.

These precise orbits are not predictions, but a-posteriori reconstructions based on GPS measurements, provided by ESA for this specific purpose, for satellites Sentinel-1A/B, Sentinel-2A/B, Sentinel-5P and Swarm-A/B/C.

Additionally, publicly available orbit predictions from the ILRS service have also been used to perform an alternative assessment. The objects are given in Table 1.

Satellite name	NORAD id
EGS(AJISAI)	16908
CRYOSAT-2	36508
GEO-IK-2	41579
JASON-3	41240
LARES	38077
LARETS	27944
PAZ	43215
SARAL	39086
STARLLETE	7646
STELLA	22824
TECHNOSAT	42829

Table 1 Considered objects with public ILRS orbits.

To validate the measurements the residuals of each plot in each track are calculated against the corresponding orbit. The S3TSR provides measurements with corrections already applied. This includes corrections due to transmitter and receiver being at different locations, equipment delays, clock drifts, light-time correction and tropospheric correction.

Influence of the ionosphere and difference between the centre of mass of the object and the surface where the signal reflects are not corrected for. The former is assumed to give very low errors while the latter depends on the size and shape of the object and its attitude, but its effect is also limited.

Therefore, the modelling for this analysis assumes purely geometrical measurements.

It has to be taken into account that the effect of the elevation in the azimuth residuals is such that for a small angular difference at high elevation the azimuth variation can be very big. To avoid this effect the azimuth residuals are multiplied by the cosine of the modelled elevation.

S3TSR accuracy has been estimated by calculating the residuals of its detections of the selected objects over a period of about 7 months.

For objects with available precise orbit, the computed residuals consistently show 95% of the values below 8 m in range, 0.5 m/s in range-rate and 0.3° in the elevation and azimuth angles, as shown in Figure 3.

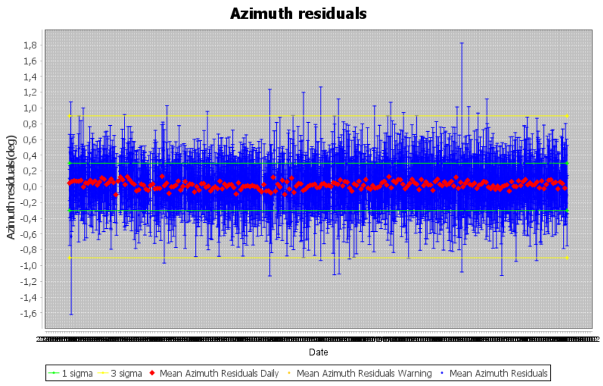

(a)

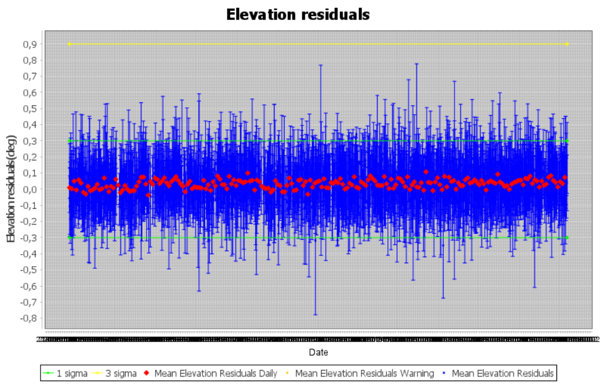

(b)

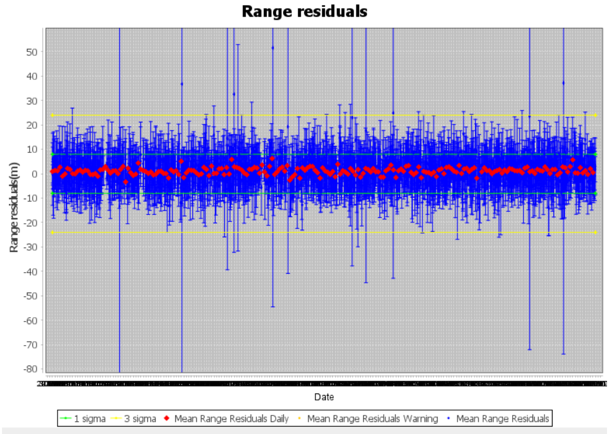

(c)

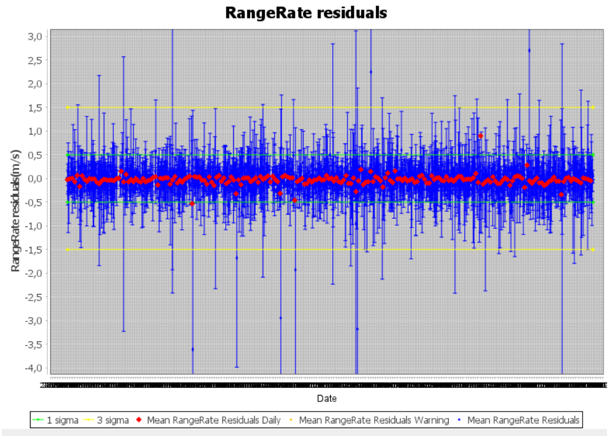

(d)

Figure 3. (a) Azimuth residuals, (b) Elevation residuals, (c) Range residuals, (d) Range rate residuals, for the objects with precise orbits.

For objects with publicly available prediction from the ILRS service, the residuals consistently show 95% of the values below 13 m in range, 0.55 m/s in range-rate and 0.4° in elevation and azimuth angles, as shown in Figure 4. The results are slightly worse because the used orbits are predictions and therefore less precise than the ESA’s a-posteriori precise orbits. Therefore, this expected result does not imply a worse performance of the radar for these objects.

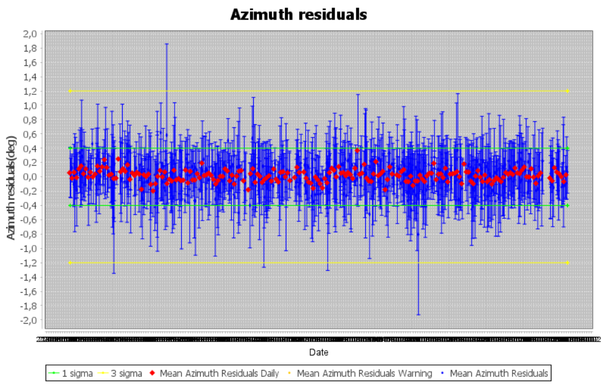

(a)

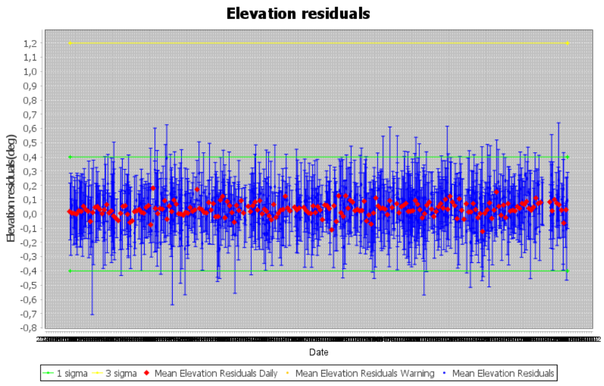

(b)

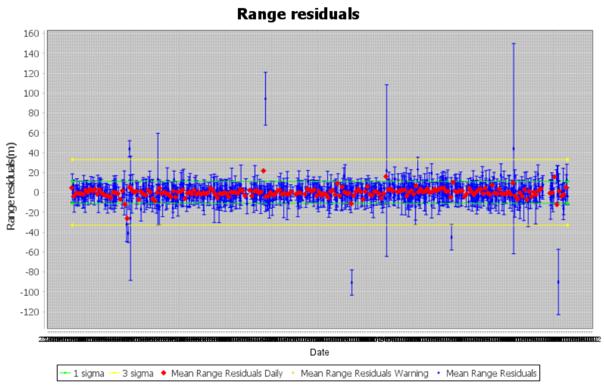

(c)

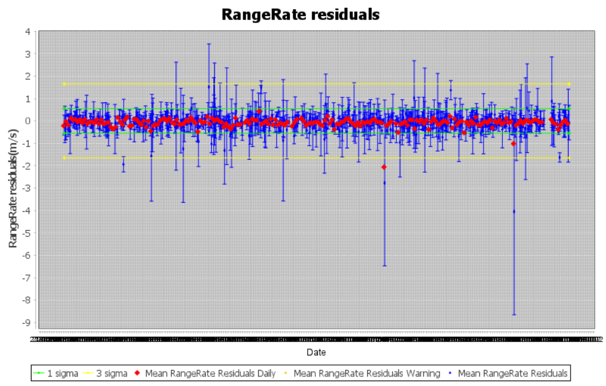

(d)

Figure 4. (a) Azimuth residuals, (b) Elevation residuals, (c) Range residuals, (d) Range rate residuals, for the objects with publicly predictions from the ILRS service.

The accuracy performance of the radar is constantly being monitored by regularly computing the residuals of the detected tracks against precise orbits for all the considered objects in a daily basis. This daily assessment shows full consistency with the accuracy estimation done in the analysis described above and allows for an early detection of possible anomalies if a degradation of the expected performance is detected.

4 DETECTION PERFORMANCE

4.1 RCS discussion

One of the topics analysed during the initial radar calibration was the assessment of the objects' Radar Cross Section (RCS) estimation. This is a quantity derived by the S3TSR from the SNR obtained for each single measurement (plot). An initial calibration was obtained during the S3TSR validation campaign by comparing the RCS at plot level and their average at track level with the theoretical value of radar calibration "spheres" of the Taifun-1 class (Figure 5), which can be easily detected by the radar. Assuming that these objects behave as Swerling-0 objects, this allowed correcting a systematic error of about 0.89 m^2.

Figure 5. Taifun-1 class spheres.

As more data was available, the analysis of the RCS estimation by the S3TSR continued. In particular, it was soon clear that Taifun-1 objects do not behave as Swerling-0 objects but rather follow a Swerling-3 distribution. In Figure 6 the distribution of the RCS from a large number of detections of Taifun-1 objects is shown, together with the Swerling-3 curve that better matches the distribution.

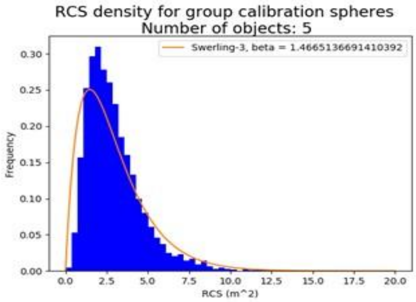

Figure 6. RCS distribution of Taifun-1 objects including the Swerling-3 curve.

An attempt to simulate the RF characteristics of the spheres was also made.

Due to lack of information on the object (materials, mechanical configuration), the object was modelled as a sphere of 2 meters in diameter with 4 linear antennas attached. The antennas are considered perfect conductors and their shape and length have been chosen based on best guesses on the base of the few available picture in relevant internet sites. In addition, conductivities and materials of the sphere's coating is based on best guesses (Figure 7).

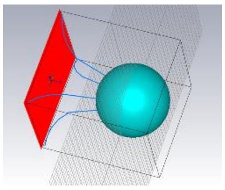

Figure 7. Mechanical model of the spheres.

Using this mechanical model, the simulation of a plane wave impinging in different angles to the sphere was performed, from which the RCS value are derived (Figure 8).

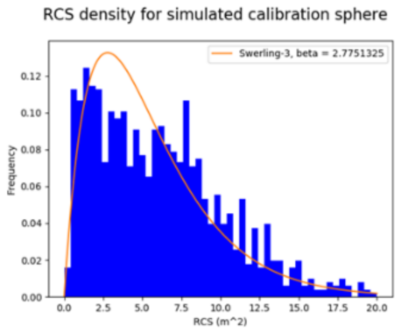

Figure 8. RCS distribution derived from the simulated calibration sphere.

The work is still in progress, but it was understood that the modelling of the Taifun-1 objects is not complete and additional and more detailed information of their physical characteristics is needed.

There are some objects more suitable for calibration than Taifun-1 objects but these are beyond the detection capability of the current configuration of the S3TSR either due to their small size or due to their altitude. The upcoming upgrade of the S3TSR will enable to detect some of these objects and the assessment of the RCS estimated by the radar will be refined.

4.2 Radar curve characterisation

The RCS-range radar curve has been derived from the measurements and the probability of detection has been calculated.

In order to do so, the theoretical probability of detection of each track is computed based on the radar cross section from previous detections for a large set of objects and the results are compared with the real detections.

To be able to compute the theoretical probability of detection for an object at a given time, we need to know its range and RCS at that time.

This theoretical probability of detection estimation at a given time can be calculated using TLE, despite the intrinsic inaccuracy of these. In this way, many more objects can be used for this analysis.

As shown in the previous section, the RCS is not a constant value for an object. Therefore, an RCS probability distribution has been derived for each object using about one year of measurements. In order to do so the RCS values measured by the S3TSR for each plot in each track correlating with that object are used, removing clear outliers that would bias the distribution.

When the object's RCS is smaller than the radar's minimum detectable RCS at the corresponding range, the plot is not detected, and therefore cannot contribute to the distribution. In order to take this into account, simulated RCS values are added between 0 (0% probability of detection) and the minimum observed RCS for the object. The number of RCS values to be added depends on the percentage of passes that are detected for the object. As an example, if the object is detected for 50% of the passes, and has been detected for 100 plots, another 100 simulated plots are added for the object.

With the derived distribution and for a given instant of time, is then easy to compute the probability of detection of a single plot as the probability that the object's RCS is greater or equal to the minimum detectable RCS at the corresponding range.

To compute the probability of detection of a track, the probability that at least 4 plots are detected is computed from the probability of individual plots separated by the scan period during the pass.

In order to derive the RCS-range curve a sweep analysis is done, where different values of minimum detectable RCS at the reference range (1000 km) are used. For each of the values the theoretical probability of detection of each track is compared with the real detections using statistical tests (z-test approximation of the binomial test) for different probability of detection intervals.

The RCS value that provides the minimum root-mean-square error with respect to the centre of the 95% confidence level interval is chosen as the minimum of the detectable RCS curve at the reference range (1000km).

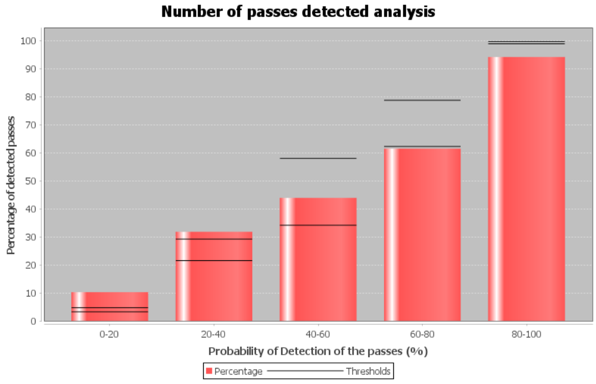

Figure 9. Example of the probability of detection analysis.

Figure 9 shows an example of output of the probability of detection analysis for a given minimum of the detectable RCS curve, showing the number of detected passes and 95% confidence intervals derived from the theoretical probability of detection computation, while Figure 10 shows the root-mean-square error for different detectable RCS values of the sweep analysis.

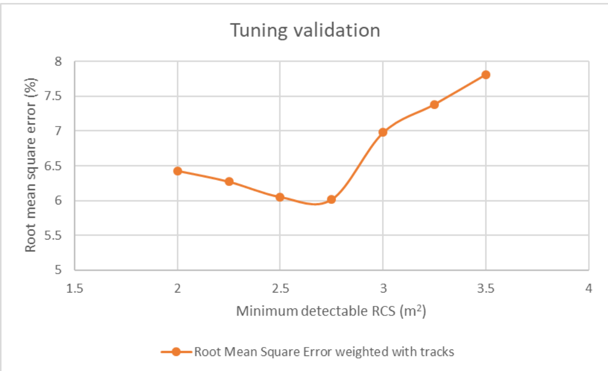

Figure 10. Root-mean-square error for each of the RCS values used in the sweep analysis.

Based on the results of the sweep analysis, the RCS that provides a minimum RMS error for an object at 1000km is 2.75 m^2.

In Figure 11 the design curve (red) and the one derived from the measurements as described above (black) are given. It can be seen that the actual performance of the radar also in terms of detection capability is meeting the initial requirement and even surpassing it.

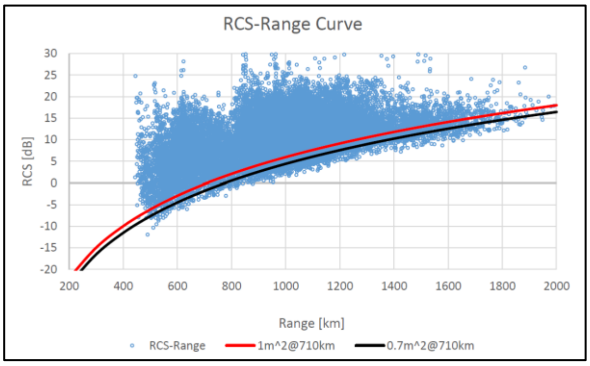

Figure 11. In red, the design RCS-Range curve and in black, the curve derived from the RCS analysis.

4.3 Radar detections evolution

The S3TSR generates currently more than 3200 tracks per 24h, relative to more than 2400 different objects in a single day. In fact, this numbers have increased in the course of these two years of operations, mainly due to the increase of the Starlink constellation. The following Figure 12 shows the evolution in the last months of the number of tracks and objects per day detected by the S3TSR.

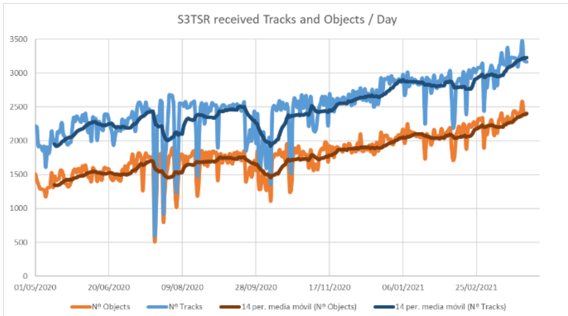

Figure 12. Radar detections evolution.

Figure 13 shows the amount of unique objects that the S3TSR detects in a single month and how it increases after Space-X launches or fragmentation such as the *NOAA 17* on the on the 10th March 2021.

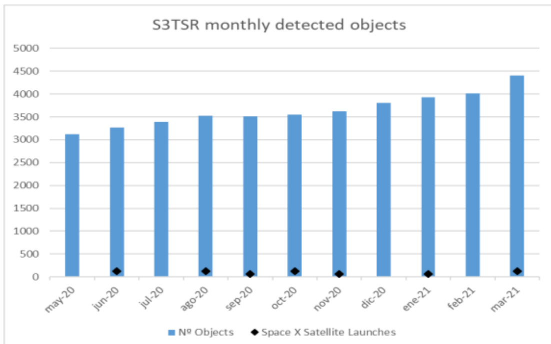

Figure 13. Monthly evolution of the S3TSR different objects detected.

In Figure 14, the number of tracks detected belonging to objects with different perigees is given. The products generated by the radar in March 2021 that correlates with the public TLE Catalogue provided by SpaceTrack are included in this analysis.

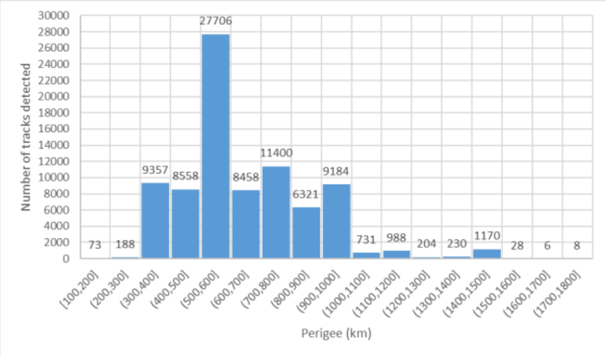

Figure 14. Number of tracks distributed over satellite perigee for March 2021.

5 MAJOR STEPS IN THE EVOLUTION OF THE S3TSR

The modular and scalable design of both Tx and Rx antennae allows the S3TSR growing in detection capability and performances. Different configurations of the S3TSR are possible, and the objective of the scalable design is to minimize downtime in operations for the current version and to re-use up to maximum the components.

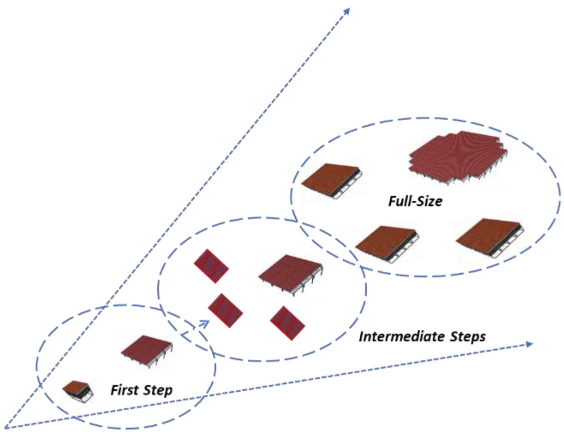

Figure 15. S3TSR upgrade path

With these two key ideas, two major configurations have been designed for the future upgrades of the radar:

- Mid term configuration foreseen by mid 2023-2024

By increasing the number of Tx up to three and enlarging the Rx, this new configurations expects to duplicate the number of objects detected and increase de detection capability up to 0.144m^2 at 1 000 Km range.

These configurations based into 3 TX buildings make use of splitting the FoR by three in order to comply with the requirement of a revisiting time of less than 10s, considered the necessary requirement to maintain a catalogue of space objects in LEO region

- Long term configuration foreseen for 2028

The S3TSR has been designed to permit the operation with up to three Tx antennas emitting double Tx beams, that is, with up to 6 simultaneous Tx beams. This is the setting required for the foreseen long term configuration (see figure 15).

By increasing the number of the building blocks composing the Rx and TX the objective is to have an increase on the detectability of 0.012 m^2 at 1 000 km range.

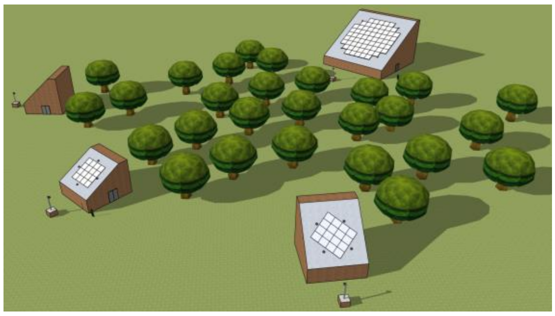

Figure 16. Illustration on long term configuration

6 CONCLUSIONS

After more than two years in operations S3TSR has proved to perform over the design objectives.

The design based on European breakthrough technology has proved to be a success. Analysis are still ongoing while the scalability of the radar as its main characteristic has allowed to draw an upgrade path that maximize the reusability of components while minimizing the downtime in operations. Two major upgrade steps will improve the surveillance capabilities in Europe for the LEO regime.

7 REFERENCES

1. Gomez, R., Salmerón, J. M. V., Besso, P., Alessandrini, M., Pinna, G. M., & Prada, M. A. R. (2019, January). Initial Operations of the Breakthrough Spanish Space Surveillance and Tracking Radar (S3TSR) in the European Context. In *1st ESA NEO and Debris Detection Conference. Presented paper. Darmstadt, Germany*.

2. Bartels, M. (2021, March 23). *Defunct US weather satellite breaks up in Earth orbit.* SPACE. https://www.space.com/defunct-weather-satellite-noaa-17-breaks-up